Understanding the evolution of anomalous anharmonicity in Bi_{2}Te_{3−x}Se_{x}

Yao Tian, Shuang Jia, R. J. Cava, Ruidan Zhong, John Schneeloch, Genda Gu, and Kenneth S. Burch

Understanding the evolution of anomalous anharmonicity in $Bi_2Te_{3-x}Se_x$

Yao Tian

Department of Physics & Institute of Optical Sciences, University of Toronto, ON M5S 1A7, Canada

Shuang Jia[*]

Department of Chemistry, Princeton University, Princeton NJ 08540, USA

Ruidan Zhong, John Schneeloch, and Genda Gu

Condensed Matter Physics & Materials Science Department, Brookhaven National Laboratory, Upton NY 11973 5000

R. J. Cava

Department of Chemistry, Princeton University, Princeton NJ 08540 ,USA

Kenneth S. Burch[†]

Department of Physics, Boston College, 140 Commonwealth Ave, Chestnut Hill MA 02467 3804, USA

(Dated: February 10, 2017)

Anharmonic effect in thermoelectrics has been a central topic for decades in both condensed matter physics and material science. However, despite the long believed strong and complex anharmonicity in the $Bi_2Te_{3-x}Se_x$ series, experimental verification of anharmonicity and its evolution with doping remains elusive. We fill this important gap with high resolution, temperature dependent Raman spectroscopy in high quality single crystals of Bi_2Te_3, Bi_2Te_2Se and Bi_2Se_3 over the temperature range from 4 K to 293 K. The Klemens's model was employed to explain the renormalization of their phonon linewidths. The phonon energy of Bi_2Se_3 and Bi_2Te_3 are analyzed in detail from three aspects, lattice expansion, cubic and quartic anharmonicity. For the first time, we explain the evolution of the anharmonicity in various phonon modes and across the series. In particular we find the interplay between cubic and quartic anharmonicity is governed by their distinct dependence on the phonon density of states, providing insights into anomalous anharmonicity designing of new thermoelectrics.

I. INTRODUCTION

The $Bi_2Te_{3-x}Se_x$ family of materials have been studied for decades as good thermoelectrics, however the physical origin of their low thermal conductivity reminds not fully understood[1]. Recently neutron scattering established anomalous anharmonicity as the origin of low thermal conductivity in another popular thermoelectric family $(Pb_{1-x}Sn_xTe)$. Specifically the anharmonicity induced softening of the transverse optic (TO) modes opens an important decay channel for one of the major heat carriers-transverse acoustic (LA) modes and thus is key to their low thermal transport[2]. First-principle studies suggest the resonant bonding mechanism is responsible for this large anharmonicity. Furthermore these studies suggest the same mechanism, although weaker, is relevant to the group V_2-VI_3 materials[3,4]. Since these materials also hold great promise for nanoelectronics due to their topological properties, understanding the evolution of anharmonicity across the $Bi_2Te_{3-x}Se_x$ series is crucial. This giant anharmonicity can also lead to new properties such as ferroelectricity[5,6], structural phase transitions[7], and reduced thermal conductivity[2]. In recent years, there has been a focus on neutron scattering as a means to explore anharmonicity, due to the emergence of new sources and excellent results in PbTe[2]. Nonetheless such studies typically require large crystals and provide large momentum but limited temperature resolution.

High resolution and small sample requirements are provided by temperature dependent Raman spectroscopy, which is well established for measuring the evolution of the lattice structure[8], phonon dynamics and anharmonicity in a wide range of materials[9–13]. While there have been some studies of $Bi_2Te_{3-x}Se_x$ using Raman spectroscopy[14,15], these either were limited to fewer phonon modes or samples were measured just at room temperature. A high temperature and spectral resolution study across the series is still lacking. Specifically, if one considers the small temperature dependent changes of phonons (typically 2-5 cm^{-1} from room temperature to 4 K) the experimental data sets obtained with different setups can be misleading. We filled this gap with the temperature dependent measurement across the whole series, performed with a single setup. In this paper, we present a Raman study of Bi_2Se_3, Bi_2Te_2Se and Bi_2Te_3 over the temperature range from 4 K to 293 K using the same Raman microscope with high spectral resolution. The anharmonicity of $Bi_2Te_{3-x}Se_x$ is discussed from two aspects. Firstly, the temperature dependence of the phonon linewidths are well explained by the Klemens's model through three-phonon interaction driven by cubic anharmonicity. Secondly, the temperature renormalization of phonon energies of Bi_2Te_3 and Bi_2Se_3 are discussed in great detail. As in most materials we find contributions to the lifetime and phonon shift from quasi-harmonic and three-phonon decay. However, in Bi_2Te_3
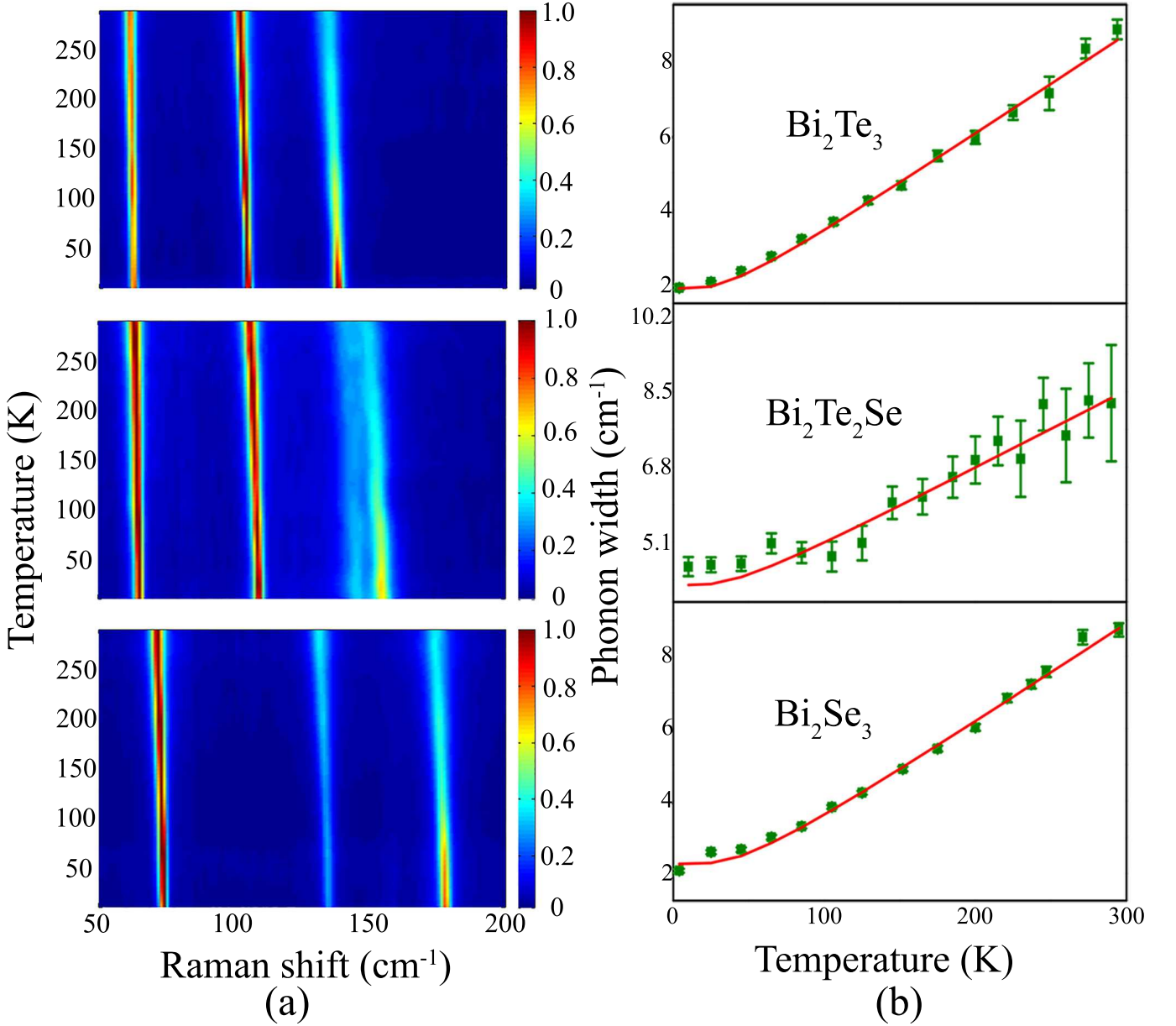
FIG. 1: a: The temperature dependent Raman spectra of $Bi_2Te_{3-x}Se_x$. From the top to the bottom are Bi_2Te_3, Bi_2Te_2Se, and Bi_2Se_3. b: The phonon linewidth of A_g^1 mode of $Bi_2Te_{3-x}Se_x$. The red lines are the anharmonic prediction. The temperature dependent renormalization of phonon linewith is relatively simple, originating from cubic anharmonicity and free of quartic anharmonicity to the lowest order.

we also find the lowest energy mode observed requires including four-phonon scattering processes that typically only emerge in materials with anomalous anharmonicity (ie. phonon modes soften as the temperature decreases, "waterfall" effect in phonon dispersion). This term usually is negligible in most materials, however has been found large and plays an important role in the strong scattering seen in IV-VI (PbTe, SnTe) materials[16] and onset ferroelectric behavior[5,6]. Furthermore we find the evolution of the strength of the anharmonic terms is easily explained in a model that accounts for the phonon density of states and joint density of states. Thus our results offer a guide for further experiments measuring and tuning the anharmonicity in materials.

II. EXPERIMENTS

The single crystals of Bi_2Se_3 and Bi_2Te_3 were grown by using a floating zone method which the melting zone was Se-rich or Te rich side. The materials of high purity 99.9999% Bi, Te and Se was pre-melted and loaded into a

10mm diameter quartz tube. The crystal growth velocity in the quartz tube was 0.5mm per hour. The Bi_2Te_2Se single crystal was grown by the Bridgeman method using special techniques to suppress carrier-concentration and the Fermi level was set inside the bulk band gap; detailed growth procedure are described in previously published work[17]. In preparation for the measurements, all single crystal samples were freshly cleaved (001 plane) and quickly placed inside a sample chamber. Exposure to air was approximately 5 minutes. The temperature dependence was achieved by an automated close-cycle cryostation designed and manufactured by Montana Instrument, Inc. The Raman spectra were taken in a backscattering configuration with a home-built Raman microscope. A linear polarized 532nm solid state laser was used as the excitation source. Signals were recorded by a cooled Andor iDus charge-coupled device (CCD). Two Ondax Ultra-narrow-band diffractive Notch Filters were used to reject Rayleigh scattering. This also allows us to observe both Stokes and anti-Stokes Raman shifts. The laser spot size was 1 micron in diameter. The laser power was kept as low as 40 μW to avoid laser-induced heating. This was checked at 4 K by monitoring the anti-Stokes signal as the laser power was reduced. Once the anti-Stokes signal disappeared, the power was cut an additional 50%. Detailed information of the instruments can be found elsewhere[18–21].

III. RESULTS AND DISCUSSION

A. Temperature Dependent Studies

For all three $Bi_2Te_{3-x}Se_x$ materials, Raman spectra were taken in the temperature range from 4 K to 293 K with 15 K steps. At each temperature, 3 acquisitions taken for 5 minutes were averaged and the spectra were corrected for the thermal factor ($n_B(\omega) + 1$, n_B is the Bose factor). The resulting temperature dependent Raman spectra are normalized to the highest phonon peak for clarity and shown in FIG. 1a. The room temperature results are consistent with previous studies[14]. Details of the group theory analysis and effects of disorder are discussed in the supplemental material. In short, three modes were observed in Bi_2Se_3 and Bi_2Te_3, we name these mode A_g^1, E_g and A_g^2 based on their symmetry. For Bi_2Te_2Se, we observed one extra mode. It turns out that the third mode (we name it V_1 mode) was ascribed to the anti-site induced local mode[11]. In all three materials, we see all phonons soften and broaden as the temperature is raised. At first glance this is not surprising since the temperature induced softening and hardening have been observed in many other materials[22,23]. However detailed analysis described in Sec. III A 2 will demonstrate qualitative differences between Bi_2Te_3 and Bi_2Se_3.

To gain more quantitative insights, we fit the Raman spectra of all three $Bi_2Te_{3-x}Se_x$ materials with the Voigt

TABLE I: Phonon frequency of $Bi_2Te_{3-x}Se_x$ at 4 K. The unit is cm^{-1}.

Material	A_g^1	E_g	V_1	A_g^2
Bi_2Te_3	62.7	104.9	–	137.6
Bi_2Te_2Se	65.1	109.1	145.1	154.7
Bi_2Se_3	73.9	134.6	–	177.7

profile function,

$$V(x, \sigma, \Omega, \Gamma) = \int_{-\infty}^{+\infty} G(x', \sigma)L(x - x', \omega, \Gamma)dx' \quad (1)$$

which is the convolution of a Gaussian and a Lorentzian. The Gaussian is employed to properly account for the instrumental resolution and the Lorentzian represents a phonon mode. The half width σ of the Gaussian was determined by the instrumental resolution, which is 1.8 cm^{-1} in our system. Three Voigt functions could be used to fit the spectra of Bi_2Te_3 and Bi_2Se_3, but four were needed for Bi_2Te_2Se. The extracted temperature dependent phonon energies ω and linewidths Γ can be used for the analysis of their anharmonicity. We also list the phonon frequencies of all modes at 4 K in Table I for a quick reference.

1. Temperature dependence of phonon linewidths

We begin by focusing on the phonon lifetime with temperature, as this typically only includes contributions from cubic terms in the anharmonicity that lead optical phonons to decay into two lower energy modes. As discussed later the phonon frequency with temperature includes this contribution as well as changes due to the lattice expansion and higher order terms in the anharmonicity. In FIG. 1b we plot the temperature dependence of the phonon scattering rate for the highest energy mode, though similar temperature dependence is seen for all modes. In all three cases the the scattering rate is well described by the Klemens's model[22] where an optical phonon is assumed to decay into two phonons with opposite momentum at half the energy of the original mode. This leads to a scattering rate described by: $\Gamma(\omega, T) = \Gamma_0 + A(2n_B(\omega/2) + 1)$, where Γ_0 results from disorder scattering, ω is the mode energy, and A is the three-phonon coupling coefficient obtained by multiplying the joint density of states by the transition matrix element. The "coalescence" process where two phonons fuse into a third is neglected, because it requires thermal populations of the second phonon which are very small at low temperatures[24]. As found in many low anharmonicity materials, the model works well for describing the lifetime[15]. In the supplemental material a detailed analysis of the lifetime of all phonons modes is provided, where we generally find an increase in A as the energy of the mode is increased. As discussed later, this is as

expected since higher energy modes typically have access to a larger phase space for decay.

2. Temperature dependence of phonon energy

As mentioned previously, the temperate dependence of the phonon energy reveals additional anharmonic effects. Typically, in a non-magnetic insulating material, the temperature dependence of a phonon energy comes from two primary sources[15],

$$\Delta\omega(T) = \Delta\omega(T)_{lattice} + \Delta\omega(T)_{anhar} \quad (2)$$

$\Delta\omega_{lattice}$ is the anharmonic correction solely due to lattice expansion, while $\Delta\omega_{anhar}$ results from the anharmonic phonon-phonon coupling. Specifically, $\Delta\omega_{lattice}$ originates from the crystal thermal expansion induced changes in the harmonic force constants and is described by the following equation for a hexagonal lattice[15],

$$\Delta\omega(T)_{lattice} = \omega(0)(e^{-\gamma \int_0^T (\alpha_c(T') + 2\alpha_a(T'))dT'} - 1) \quad (3)$$

where γ is the mode Grüneisen parameter, and α_a and α_c are the coefficients of linear thermal expansion along the a and c axes. The Grüneisen parameters describe the effect that the volume change of a crystal lattice has on its vibrational properties and its value varies for different phonon modes. In most analysis, the mode-averaged Grüneisen parameter is typically used to characterize the volume change induced phonon frequency shifts since it is relatively easy to obtain by comparing the specific heat to the lattice expansion[15]. However, to truly understand the anharmonicity in these materials it is crucial to evaluate each mode separately. Indeed, the relationship of each mode to the lattice expansion can be quite distinct, especially in thermoelectric materials[3]. Thus, in the following discussion we use mode Grüneisen parameter to capture the phonon frequency shifts induced by thermal expansion. To the best of our knowledge, the relevant data to calculate $\Delta\omega_{lattice}$ is absent for Bi_2Te_2Se. Thus, Bi_2Te_2Se is omitted for the discussion here.

On the other hand, $\Delta\omega_{anhar}$ arises from the coupling of phonon modes through the cubic and quartic anharmonicity[25],

$$\Delta\omega(T)_{anhar} = \frac{12}{\hbar} \sum_{\vec{q},j_1} V \begin{pmatrix} 0 & 0 & \vec{q} & -\vec{q} \\ j & j & j_1 & j_1 \end{pmatrix} (2n_B(\vec{q},j)+1)$$
$$- \frac{18}{\hbar} \sum_{\vec{q},j_1,j_2} |V \begin{pmatrix} 0 & \vec{q} & -\vec{q} \\ j & j_1 & j_2 \end{pmatrix}|^2 R(\omega) \quad (4)$$

$$R(\omega) = \frac{n_B(\vec{q},j_1) + n_B(-\vec{q},j_2) + 1}{\omega - \omega(\vec{q},j_1) - \omega(-\vec{q},j_2)} \quad (5)$$

where V are the coefficients derived from the lattice potential energy of deformation at constant volume, and q and j are momentum and band index respectively. We can see that equation 4 has two parts: the quartic anharmonicity (the first term of equation 4) to first order in the perturbation theory and cubic anharmonicity (the second term of equation 4) to second order. As described above, the cubic anharmonicity term contributes to the phonon linewidth as well. The quartic anharmonicity to first order only contributes to the phonon frequency, thus showing the importance of analyzing both the lifetime and frequency of the modes versus temperature. In most cases, the cubic anharmonicity dominates and results in softening and broadening the phonon as the temperature rises[12]. However, for materials with high anharmonic potentials (e.g. ferroelectrics), the quartic term plays a significant role[6,26]. Therefore, it is worthy to disentangle the relative contributions from the cubic and quartic anharmonicity in Bi_2Se_3 and Bi_2Te_3. To achieve this, one has to first remove the effect of $\Delta\omega_{lattice}$. To do this we first determined the mode Grüneisen parameters from previous measurements of the pressure dependence (see the supplemental material) as well as established thermal expansion coefficients[27,28]. Our main conclusion is not strongly affected by a change of 20 % change of these parameters. Next we used equation 3 to calculate the $\Delta\omega_{lattice}$ for Bi_2Se_3 and Bi_2Te_3.

Before proceed further, we notice from equation 4 that both the cubic and quartic anharmonic terms also contribute to the phonon frequency at zero temperature. However, it is difficult to unambiguously distinguish whether the resulted phonon frequency shifts are from harmonic or anharmonic components without a detailed first-principle calculation which is beyond the scope of this paper. Thus, we decide to focus on the temperature dependent shifts of the phonon mode frequencies in the following discussion. In FIG. 2 we plot $\Delta\omega(T) = \omega(T) - \omega(4\ K)$. In addition we also show the calculated lattice contribution $\Delta\omega_{lattice}$, and the anharmonic component obtained by subtracting the lattice contribution from the measured data ($\Delta\omega_{anhar}' = \Delta\omega(T) - \Delta\omega_{lattice}$). Here $\Delta\omega_{anhar}'$ is just $\Delta\omega_{anhar}$ with the temperature independent constant removed which is expressed by the following formula:

$$\Delta\omega(T)_{anhar}' = \frac{12}{\hbar} \sum_{\vec{q},j_1} V \begin{pmatrix} 0 & 0 & \vec{q} & -\vec{q} \\ j & j & j_1 & j_1 \end{pmatrix} 2n_B(\vec{q},j)$$
$$- \frac{18}{\hbar} \sum_{\vec{q},j_1,j_2} |V \begin{pmatrix} 0 & \vec{q} & -\vec{q} \\ j & j_1 & j_2 \end{pmatrix}|^2 R(\omega)'$$
$$(6)$$

$$R(\omega)' = \frac{n_B(\vec{q},j_1) + n_B(-\vec{q},j_2)}{\omega - \omega(\vec{q},j_1) - \omega(-\vec{q},j_2)} \quad (7)$$

Focusing first on Bi_2Te_3 in FIG. 2a-c, we see the $\Delta\omega_{anhar}'$ for the A_g^1 mode (FIG. 2a) almost stays at zero between 4 K to 175 K and slowly hardens at the higher temperature. For the E_g (FIG. 2b) and A_g^2 (FIG. 2c) modes the $\Delta\omega_{anhar}'$ is monotonically decreasing through-
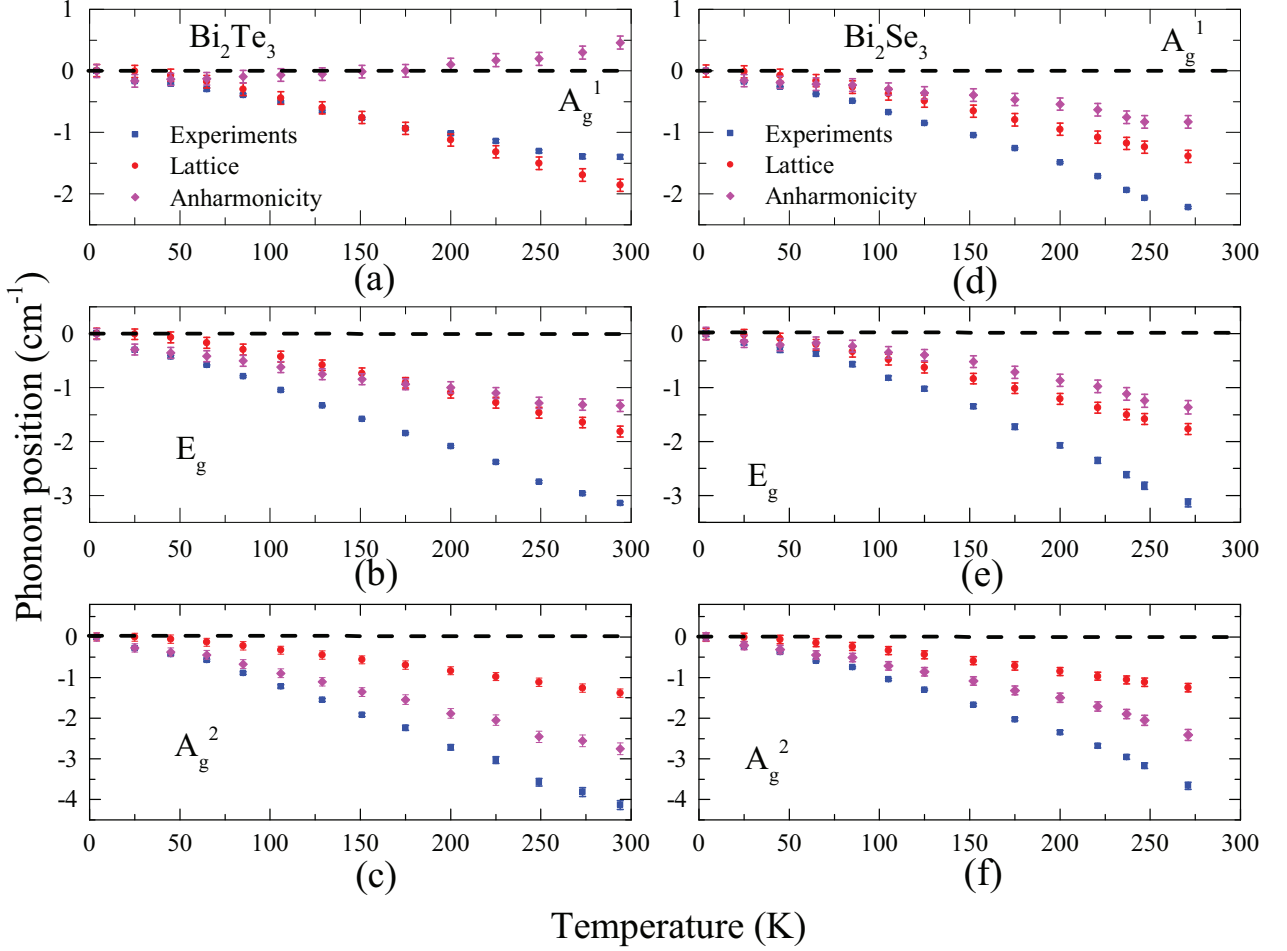
FIG. 2: Temperature dependence of phonon frequency of Bi_2Te_3 (a-c) and Bi_2Se_3 (d-f). All data points are offset by the phonon frequency at lowest temperature. The dash line indicates zero offset. We notice that the anharmoncity induced phonon energy shifts are dramatically different between the A_g^1 mode of Bi_2Te_3 (hardening) and that of Bi_2Se_3 (softening). This is explained by the anomalous quartic anharmonicity in Bi_2Te_3 which is absent in Bi_2Se_3. Besides, as the phonon energy increases in Bi_2Te_3, the trend switches sign from hardening to softening due to the relative contributions from phonon joint density of states and density of states. Detailed discussion can been seen in the texts.

out the entire temperature range and increases in magnitude as the phonon frequency increases. For example at 300 K, $\Delta\omega_{anhar}'$=1.2 cm^{-1} for E_g, while $\Delta\omega_{anhar}'$=2.5 cm^{-1} for the A_g^2 mode. To understand this strikingly different behavior of the modes, let us re-examine the different contributions to the anharmonicity. According to equation 6, the anharmonicity interaction contributes two terms: the cubic and quartic anharmonicity with different signs. These two terms can cause a phonon mode to soften or harden as the temperature increases depending on their relative magnitudes. Moreover, the strength of the two terms increases at different rates as the phonon frequency increases. Apparently, the cubic term is dominant in the E_g and A_g^2 modes, leading to $\Delta\omega_{anhar}'$ softening the mode as the temperature is increased. However,

the case for the A_g^1 mode is complicated. To explain the behavior of this mode, let us delve into equation 6 again. According to equation 6, both cubic and quartic anharmonic terms are functions of the Bose factor $n_B(\hbar\omega/kT)$. This is a nonlinear function and increases very slowly at the low temperatures. In the ideal scenario, we expect to observe a curve that starts from zero with a flat slope at the lowest temperatures and becomes larger at high temperatures. However, given the small amplitude of the difference in the anharmonic contributions from quartic and cubic anharmonicity and the spectral resolution of our Raman microscope, the data we obtained is almost zero in the temperature range between 4 K to 175 K. Nevertheless, in the temperature range from 200 K to 290 K where the Bose factor becomes more significant we can

clearly see the hardening trend. Thus, we conclude that the quartic term is slightly larger for this mode.

To understand how the $\Delta\omega_{lattice}'$ evolves with the phonon frequency and the difference between the cubic and quartic anharmonicity, let us revisit the two anharmonic terms in equation 6. The sum (one band index j_1) in the quartic term of equation 6 is proportional the one phonon density of states ($D(\omega)$) and that in the cubic term (two band indexes j_1, j_2) is proportional to the joint two-phonon density of states ($JD(\omega)$). For simplification, one can approximate $JD(\omega)$ as $D(\omega-\omega_1)\times D(\omega_1)$ where $\omega-\omega_1$ and ω are the energy of the two phonon modes respectively. For a qualitative understanding $JD(\omega)$ can be further simplified using Klemens's approximation where $\omega_1 = \omega/2$. Thus, eventually $JD(\omega)$ takes the form $D(\omega/2)^2$. As a result, the quartic (cubic) term is proportional to $D(\omega)$ $(D(\omega/2)^2)$. In a simple picture where optical mode interacts with an acoustic mode, $D(\omega)$ increases monotonically with ω. If the phonon frequency ω is small, it is possible that $D(\omega)$ is equal to or larger than $JD(\omega)$. In the meanwhile, if the quartic anharmonic coefficient ($V\begin{pmatrix} 0 & 0 & \vec{q} & -\vec{q} \\ j & j & j_1 & j_1 \end{pmatrix}$) is reasonably large, it can be expected that the quartic term wins and results in a hardening of phonon energy as the temperature increases, which is the case for the A_g^1 mode. As the phonon frequency increases, $JD(\omega)$ increases much faster than $D(\omega)$. Therefore, in the E_g and A_g^2 modes negative $\Delta\omega_{anhar}'$ is observed and becomes larger in magnitude from the E_g mode to the A_g^2 mode. At this point, it may be worthy to compare the behavior of the A_g^1 mode with the standard ferroelectrics, as we mentioned previously that the quartic anharmonicity there plays a key in the tuning the phonon frequency shifts[6]. Compared to the soft modes in standard ferroelectrics such as $SrTiO_3$ and $BaTiO_3$, the magnitude that the A_g^1 mode hardens as the temperature is raised is small and in order to see the hardening, $\Delta\omega_{lattice}$ has to be subtracted. However, the temperature dependent behaviors are similar where the phonon frequencies harden and linewidths broaden as the temperature increases[29,30]. The small magnitude we observed may be due to the energy of the A_g^1 mode being comparatively high and the quartic anharmonic term balanced to a large extent by the cubic anharmonic term. The statements above are also evidenced by the fact that the IR-active E_u mode, whose energy is lower than all three Raman-active modes, seems hardens from 48 cm^{-1} to 50 cm^{-1} from 15 K to 300 K even without the subtraction of $\Delta\omega_{lattice}$[14].

To further explore the role of phonon frequency in the strength of the anharmonicity, we now turn to Bi_2Se_3, where the modes are at higher frequencies. Specifically, for Bi_2Se_3 a similar analysis was performed and the results are shown in FIG. 2d-f. We find that the thermal expansion contribution term $\Delta\omega_{lattice}$ accounts for 63%, 57% and 34% of the total phonon frequency shift at room temperature for each mode, respectively. In the case of Bi_2Se_3, the resulting $\Delta\omega_{anhar}'$ are all negative.

The magnitude of $\Delta\omega_{anhar}'$ increases monotonically from 0.7 cm^{-1} (A_g^1, FIG. 2d), 1.2 cm^{-1} (E_g, FIG. 2e) to 2.5 cm^{-1} (A_g^2, FIG. 2f) at 295 K. This suggests the quartic term is smaller and the cubic terms are dominating in all three modes.

At this point one may wonder whether it is simply the change in the density of states with phonon energy that results in the dramatic difference in the temperature dependence of the lowest energy phonon in $Bi_2Te_{3-x}Se_x$. In fact we have so far ignored contributions from the strength of the potential and resulting changes in the matrix elements. This is likely to play a large role as the lowest energy Raman mode in Bi_2Se_3 that we observe is only 11 cm^{-1} higher than the equivalent mode in Bi_2Te_3. One explanation for the dramatic difference may be the resonant bonding theory, where the long-ranged interaction from the neighbors to the atomic potential lead to anomalous anharmonicity[3,31–33]. Indeed this mechanism has been suggested to be responsible for the low thermal conductivity of Bi_2Te_3[3]. As described in the supplemental material a simple calculation suggests the resonant bonding should be stronger in Bi_2Te_3 than Bi_2Se_3. The reason for the difference can be understood as the p-electron in Te atoms are more delocalized than those in Se atoms. Nonetheless the detailed first principle calculations of Bi_2Se_3 required to confirm this suggestion are beyond the scope of this paper.

As we mentioned earlier, the decay channel $LA+TO \rightarrow TO$ plays a significant role in the lowering the thermal conductivity in thermoelectric materials . Interestingly, a very similar phonon decay channel $TA + TO \rightarrow TO$ was found in perovskite ferroelectrics which also been attribute to lowering the thermal conductivity[34,35]. The common feature in these two types of materials is that the TO mode significantly softens as the temperature is lowered. We have shown that the anharmonicity in Bi_2Te_3 similarly softens the A_g^1 mode. However, its energy is much higher than the TO modes in the perovskite ferroelectrics[34] and $PbTe$[2], so the contribution to the scattering of LA in Bi_2Te_3 is probably small. As we pointed out in the supplemental material, the first E_g mode of $Bi_2Te_{3-x}Se_x$ is near 30 cm^{-1}[14,36,37] which is very close in energy to the soft TO modes in other highly anharmonic materials. Thus it will be extremely helpful in future studies to carefully examine the temperature dependence of this mode.

IV. CONCLUSIONS

In summary, we have performed high resolution, temperature dependent Raman scattering measurements on Bi_2Te_3,Bi_2Te_2Se and Bi_2Se_3. These Raman results of the $Bi_2Te_{3-x}Se_x$ provide experimental insights into the long standing problem: the origin of the complex anharmonicity as the chalcogenide and/or the energy of the mode is changed.

Through the analysis of temperature dependent

phonon energy, we found the quartic anharmonicity is the key to explain the temperature dependent phonon frequency shifts of A_g^1 mode for Bi_2Te_3 which is less significant in Bi_2Se_3. Besides, the complex temperature and phonon energy dependent phonon frequency shifts can be primarily explained by the competition between quartic and cubic anharmonic terms. These two terms are dependent on the one and two-phonon density of states respectively, which grow at different rates. As such, our observations that a positive $\Delta\omega_{anhar}'$ for A_g^1 mode in Bi_2Te_3, a sign switch and a growth in amplitude of $\Delta\omega_{anhar}'$ are all consistent with this picture. However, it may be that the change in density of states of the phonons is not enough to explain the difference, and thus our results may provide evidence for the resonant bonding in Bi_2Te_3 and its weaker role in Bi_2Se_3.

While these results clearly show the role of the chalcogenide in enhancing resonant bonding and tuning the anharmonicity in $Bi_2Te_{3-x}Se_x$, further experimental and theoretical efforts are required to fully understand how the anharmonicity, crucial to their thermal and lattice properties, is tuned.

[*] Current address: School of Physics, Peking University, Beijing, China, 100871
[†] ks.burch@bc.edu
[1] H. J. Goldsmid, *Introduction to thermoelectricity*, Vol. 121 (Springer Science & Business Media, 2009).
[2] O. Delaire, J. Ma, K. Marty, A. F. May, M. A. McGuire, M.-H. Du, D. J. Singh, A. Podlesnyak, G. Ehlers, M. Lumsden, *et al.*, Nature materials **10**, 614 (2011).
[3] S. Lee, K. Esfarjani, T. Luo, J. Zhou, Z. Tian, and G. Chen, Nature Communications **5** (2014).
[4] O. Hellman and D. A. Broido, Physical Review B **90**, 134309 (2014).
[5] I. Katayama, H. Aoki, J. Takeda, H. Shimosato, M. Ashida, R. Kinjo, I. Kawayama, M. Tonouchi, M. Nagai, and K. Tanaka, Physical review letters **108**, 097401 (2012).
[6] R. Cowley, Reports on progress in physics **31**, 123 (1968).
[7] K. Fujii, Y. Aikawa, and K. Ohoka, Physical Review B **63**, 104107 (2001).
[8] M. Huang, H. Yan, T. F. Heinz, and J. Hone, Nano letters **10**, 4074 (2010).
[9] A. Hushur, M. H. Manghnani, and J. Narayan, Journal of Applied Physics **106**, 054317 (2009).
[10] T. Oznuluer, E. Pince, E. O. Polat, O. Balci, O. Salihoglu, and C. Kocabas, Applied Physics Letters **98**, 183101 (2011).
[11] Y. Tian, G. B. Osterhoudt, S. Jia, R. Cava, and K. S. Burch, Applied Physics Letters **108**, 041911 (2016).
[12] J. Lin, L. Guo, Q. Huang, Y. Jia, K. Li, X. Lai, and X. Chen, Physical Review B **83**, 125430 (2011).
[13] Y. Tian, M. J. Gray, H. Ji, R. J. Cava, and K. S. Burch, 2D Materials **3**, 025035 (2016).
[14] W. Richter and C. R. Becker, Physica Status Solidi B **84**, 619 (1977).
[15] Y. Kim, X. Chen, Z. Wang, J. Shi, I. Miotkowski, Y. P. Chen, P. A. Sharma, A. L. Lima Sharma, M. A. Hekmaty, Z. Jiang, and D. Smirnov, Applied Physics Letters **100**, 071907 (2012).
[16] Y. Chen, X. Ai, C. Marianetti, *et al.*, Physical review letters **113**, 105501 (2014).
[17] S. Jia, H. Ji, E. Climent-Pascual, M. Fuccillo, M. Charles, J. Xiong, N. Ong, and R. Cava, Physical Review B **84**, 235206 (2011).
[18] L. Sandilands, J. Shen, G. Chugunov, S. Zhao, S. Ono, Y. Ando, and K. Burch, Physical Review B **82**, 064503 (2010).
[19] C. Beekman, A. Reijnders, Y. Oh, S. Cheong, and K. Burch, Physical Review B **86**, 020403 (2012).
[20] L. J. Sandilands, Y. Tian, K. W. Plumb, Y.-J. Kim, and K. S. Burch, Physical Review Letters **114**, 147201 (2015).
[21] Y. Tian, A. A. Reijnders, G. B. Osterhoudt, I. Valmianski, J. Ramirez, C. Urban, R. Zhong, J. Schneeloch, G. Gu, I. Henslee, *et al.*, Review of Scientific Instruments **87**, 043105 (2016).
[22] P. G. Klemens, Physical Review **148**, 845 (1966).
[23] J. Menéndez and M. Cardona, Physical Review B **29**, 2051 (1984).
[24] S. Usher and G. Srivastava, Physical Review B **50**, 14179 (1994).
[25] R. Lowndes, Physical Review B **6**, 1490 (1972).
[26] F. Jona and G. Shirane, *Ferroelectric crystals*, Vol. 1 (Pergamon, 1962).
[27] X. Chen, H. Zhou, A. Kiswandhi, I. Miotkowski, Y. Chen, P. Sharma, A. L. Sharma, M. Hekmaty, D. Smirnov, and Z. Jiang, Applied Physics Letters **99**, 261912 (2011).
[28] L. M. Pavlova, Y. I. Shtern, and R. E. Mironov, High Temperature **49**, 369 (2011).
[29] V. Denisov, B. Mavrin, V. Podobedov, and J. Scott, Journal of Raman spectroscopy **14**, 276 (1983).
[30] K. Inoue, A. Hasegawa, K. Watanabe, H. Yamaguchi, H. Uwe, and T. Sakudo, Physical Review B **38**, 6352 (1988).
[31] D. Lencer, M. Salinga, and M. Wuttig, Advanced Materials **23**, 2030 (2011).
[32] T. Matsunaga, N. Yamada, R. Kojima, S. Shamoto, M. Sato, H. Tanida, T. Uruga, S. Kohara, M. Takata, P. Zalden, *et al.*, Advanced Functional Materials **21**, 2232 (2011).
[33] C. Li, J. Hong, A. May, D. Bansal, S. Chi, T. Hong, G. Ehlers, and O. Delaire, Nature Physics (2015).
[34] H. Barrett and M. Holland, Physical Review B **2**, 3441 (1970).

[35] M. Tachibana, T. Kolodiazhnyi, and E. Takayama-Muromachi, Applied Physics Letters **93**, 92902 (2008).

[36] V. Gnezdilov, Y. G. Pashkevich, H. Berger, E. Pomjakushina, K. Conder, and P. Lemmens, Physical Review B **84**, 195118 (2011).

[37] H. Shi, D. Parker, M.-H. Du, and D. J. Singh, Physical Review Applied **3**, 014004 (2015).